In-situ characterization of the near-surface small strain damping ratio at the Garner Valley Downhole Array through surface waves analysis

Mauro Aimar[1*][0000-0002-1170-9774], Mauro Francavilla[1], Brady R. Cox[2][0000-0001-8022-9822] and Sebastiano Foti[1][0000-0003-4505-5091]

[1] Politecnico di Torino, Corso Duca degli Abruzzi 24, 10129 Torino, Italy
[2] Utah State University, 84322 Logan, USA
mauro.aimar@polito.it

Abstract. The proper quantification of the small strain damping ratio has great relevance in geotechnical earthquake engineering. This parameter is generally obtained from either direct laboratory tests on small samples or generic empirical relationships. Alternatively, some promising techniques for extracting in-situ small strain damping ratio rely on the analysis of surface wave data. This paper presents a subset of results from a massive dynamic site characterization study at the Garner Valley Downhole Array, wherein in-situ damping ratio profiles have been extracted from several multichannel analysis of surface waves (MASW) datasets. Waveforms generated from both a sledgehammer and a dynamic shaker were recorded, allowing for comparisons between the damping estimates obtained from both types of sources. Dispersion data and attenuation curves were derived from the waveforms using several approaches presented in the literature, and one new approach developed by the authors. This paper documents the inter-method differences and similarities across approaches in terms of uncertainties in the wavefield attenuation, together with the impacts on the amplification of the soil deposit. This study contributes towards better, in-situ characterization of the attenuation properties of soil deposits, enhancing the accuracy of ground models used in dynamic analyses. It is expected that progress in this area will lead to greater reliability of predicted ground motion amplification.

Keywords: Small Strain Damping Ratio, Surface Waves, MASW, Uncertainties.

1 Introduction

A proper evaluation of site effects is crucial to define the expected ground motion at the surface. Among the various parameters affecting the stratigraphic amplification, the soil small-strain damping ratio D_0 and the related uncertainties are gaining attention. This parameter, in fact, is believed to control variations in motion amplitude and frequency content, especially when a low-intensity shaking is involved (e.g., [1]).

The D_0 is typically estimated from laboratory tests. However, experimental evidence from back-analysis of Down-Hole seismic arrays showed D_0 values in the field larger

than the ones obtained through laboratory tests. In fact, at the site scale, complex wave propagation phenomena (e.g., wave scattering [2]) induce additional energy dissipation to the material dissipation that cannot be captured by laboratory tests. Therefore, an in-situ estimate of D_0 should be adopted in ground response simulations.

A potentially effective way for obtaining soil dissipative parameters relies on geophysical tests, especially on Multi-Channel Analysis of Surface Waves (MASW). The MASW-based estimate of the shear-wave velocity V_S and D_0 refers to the measurement of variations of phase and amplitude of surface waves along linear arrays with active sources, from which the dispersion and the attenuation curves are obtained. These curves describe variations of the Rayleigh wave phase velocity and the phase attenuation with the frequency. This dependence is the combined effect of both geometrical dispersion, i.e. the variation in mechanical properties with depth, and intrinsic dispersion, linked to the frequency-dependence of material parameters in linear, viscoelastic media (e.g., [3]). Then, the V_S and D_0 profiles are estimated through an inversion scheme, where a theoretical soil model is calibrated to match the experimental dispersion and attenuation data.

This note shows some relevant results of a MASW survey performed at the Garner Valley Downhole Array (GVDA) site, utilizing a sledgehammer and a vibroseis truck as active sources. Experimental dispersion and attenuation curves were obtained according to different methods, and results were compared to highlight strengths and limitations of each one. Furthermore, the influence of source characteristics on the quality of estimated data was investigated. The second part of the paper focuses on the inversion problem for the coupled estimation of the V_S and D_0 profiles, that are compared with results from other geophysical surveys. The corresponding amplification is finally computed and compared with the one obtained from observed data, to check the reliability of the derived soil models in capturing the site response.

2 Site description and data acquisition

The Garner Valley Down-Hole Array is a site located in Southern California. The site stratigraphy is characterized by alluvial soil with a shallow water table, that overlies a layer of decomposed granite transitioning to competent granite bedrock. This site is instrumented with a seismic monitoring system. The equipment includes an instrumented borehole, with accelerometers on the surface and at various depths, to capture variations in the ground motion in the soil deposit. For this reason, the site represents an effective benchmark for testing the validity of ground motion amplification models.

The investigation of the small-strain parameters of the soil deposit at the GVDA site was carried out by means of a MASW survey. The testing involved a two-dimensional array (Fig. 1), made by a regular grid of geophones, to develop a three-dimensional model of the soil deposit. This study, however, focuses on the South-East line, which is a linear array composed by 14 geophones, with inter-receiver distance equal to 5 m. The receivers are Magseis Fairfield Nodal ZLand 3C sensors, that are three-component geophones suitable for both active and passive surveys. Waveform were generated through the NHERI@UTexas Thumper vibroseis truck [4] and an instrumented

sledgehammer. The shaker generated a chirp signal, with frequency content ranging between 5 Hz and 30 Hz, at two shot points with reversal. The source-offsets of road-side shot points are 4.5 m and 35.5 m respectively, whereas the ones on the parking side are 2.5 m and 33.5 m far from the closest sensor. As for the sledgehammer, two source-offsets of 5 m and 15 m were used off both ends.

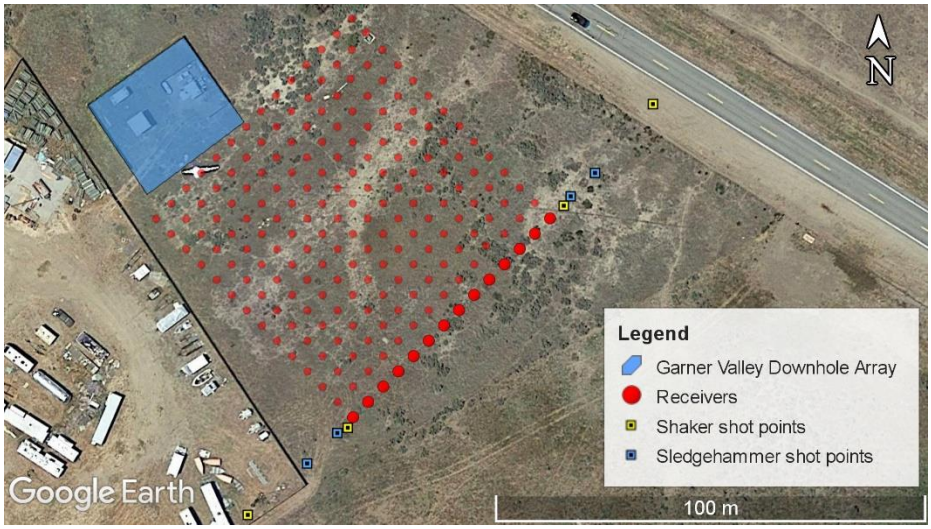

Fig. 1. MASW array setup. The larger circles represent the receivers belonging to the array analyzed in this study. The blue area identifies GVDA, where the instrumented boreholes are located.

3 Data processing

The estimation of the Rayleigh phase velocity V and phase attenuation α was carried out by using different methods. For simplicity, this section compares results from shaker data, and the influence of source characteristics will be reported later.

The considered methods are the Transfer Function Method (TFM) [3], the Generalized Half-Power Bandwidth Method (GHPB) [5] and the Wavefield Decomposition Method (WD) [6]. In addition, this study considers a new technique, i.e. the Frequency-Domain BeamForming – Attenuation (FDBFa) [7]. This approach is a generalization of the Frequency-Domain BeamForming (FDBF) method [8] for the attenuation estimate and it is based on the following wavefield transformation:

$$v(r,\omega)=[u(r,\omega)]^{j} \tag{1}$$

where $u(r,\omega)$ is the particle displacement (as a function of the distance r and the circular frequency ω) and j is the imaginary unit. In the case of a single dominant mode, it can be demonstrated that the wavenumber of the transformed wave $v(r,\omega)$ corresponds to the attenuation of the original one [7]. Hence, α can be estimated through the dispersion analysis of $v(r,\omega)$ – in this case, by using the FDBF approach. In the

estimation, the geometric spreading effect on the wave amplitude is removed by multiplying recorded data by $\sqrt{r}$ (e.g., [3]).

Fig. 2 compares the dispersion and attenuation curves obtained for each method. Results are described in terms of mean μ and coefficient of variation (CoV), i.e. the ratio between the standard deviation and μ. Data statistics were estimated through the multiple source-offset technique [9]. In all the cases, only the fundamental mode was identified. The dispersion curves are rather close to each other and affected by low variability, for almost each approach. As for α, all the approaches agree quite well at short wavelengths, although the WD scheme is not able to estimate wave parameters at wavelengths greater than 30 m, for this site. On the other side, the TFM matches the average values of all the other methods, even with less variability. However, it tends to overestimate α at greater wavelengths, probably because of near-field effects, that are not modeled in this case. Finally, the GHPB and the FDBFa methods provide similar results, though the former is affected by rather large variability both on V and α.

As for the source effect, Fig. 3 compares the normal statistics of the estimated V and α from shaker data and sledgehammer data. For simplicity, only results derived through the FDBFa method are considered, but similar considerations are valid for the other methods. The mean estimates are close to each other, independently from the investigated wavelength. However, shaker data extend to longer wavelengths. Furthermore, sledgehammer-based α is affected by larger variability, differently from V. A potential reason of the different scatter might be noise, as the sledgehammer is not a high-energy source and the signal-to-noise ratio of recorded traces might be low, especially at high frequencies. However, the mean trend in the attenuation curve can still be captured.

4 Data inversion

The estimated V and α data were used to estimate the V_S and D_0 profiles, through a joint inversion of the experimental curves. For simplicity, the analysis focused on results from shaker data, interpreted according to the FDBFa method.

The inversion was carried out by using a Monte-Carlo-based global search algorithm. The algorithm is based on a smart sampling technique of the model parameter space, by exploiting the scaling properties of the modal curves [7; 10]. Thus, a good quality result can be achieved with a moderately small number of generated ground models. The randomization of earth models investigated an adequate range of layer thicknesses, S-wave velocities and damping ratios, whereas P-wave velocities and mass densities were inferred from borehole logs [11]. Instead, the P-wave damping ratio was kept equal to the corresponding one for S-waves. Forward dispersion and attenuation modeling was carried out through the ElastoDynamics Toolbox [12].

The degree of matching between synthetic and experimental data is measured through the following misfit function:

$$M = \frac{1}{2n}\left[\sum_{i=1}^{n}\frac{\left(V_{t,i}-V_{e,i}\right)^2}{\sigma_{V,i}^2}+\sum_{i=1}^{n}\frac{\left(\alpha_{t,i}-\alpha_{e,i}\right)^2}{\sigma_{\alpha,i}^2}\right] \tag{2}$$

where $V_{t,i}$ and $V_{e,i}$ are the theoretical and experimental velocity values and $\sigma_{V,i}$ is the corresponding standard deviation, $\alpha_{t,i}$, $\alpha_{e,i}$ and $\sigma_{\alpha,i}$ are the corresponding ones for phase attenuation and n is the number of sample points in the experimental data.

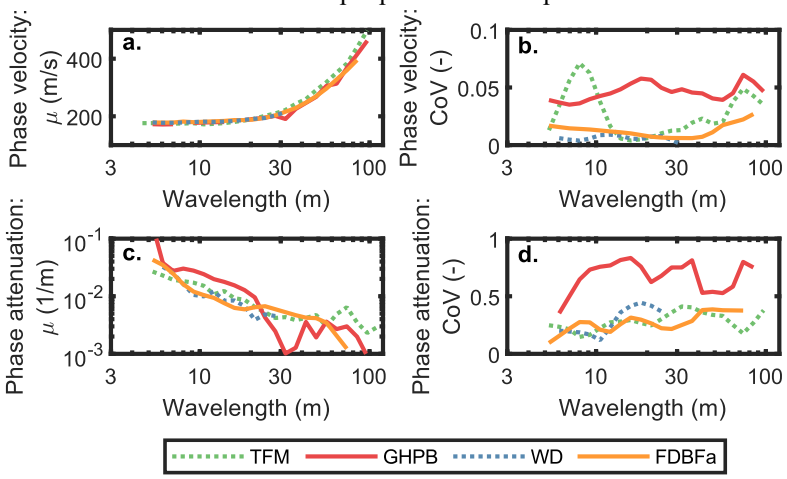

Fig. 2. Inter-method comparison: a) mean and b) coefficient of variation of the estimated phase velocity; c) mean and d) coefficient of variation of the estimated phase attenuation.

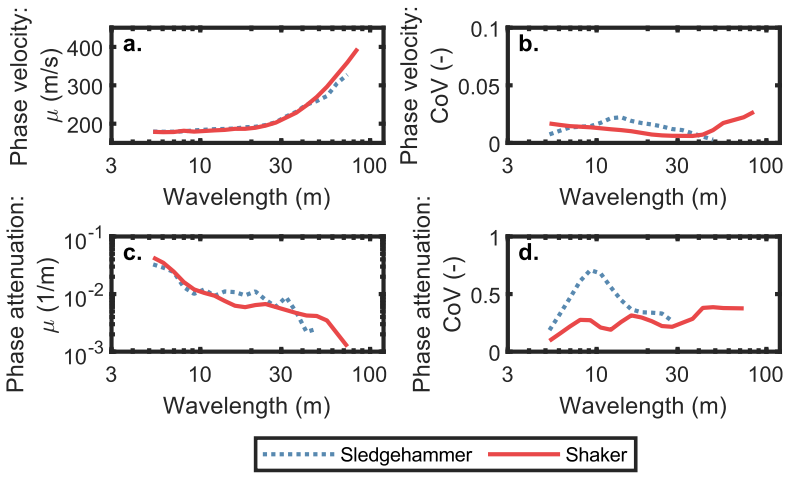

Fig. 3. Influence of source characteristics: a) mean and b) coefficient of variation of the estimated phase velocity; c) mean and d) coefficient of variation of the estimated phase attenuation.

Fig. 4 shows results for the best fitting 10 models out of 10,000 trial profiles. Inverted V_S profiles are poorly scattered, whereas D_0 profiles are affected by large variability. This is an effect of the high CoV in the experimental attenuation data, that does not allow an effective constraint of D_0. For comparison purposes, Fig. 4 includes profiles obtained from P-S suspension logging [11] and a Down-Hole test [13], where the corresponding D_0 was estimated through Darendeli's empirical relationship [14]. Resulting

profiles are quite compatible with each other, although MASW-based D_0 rises up to 5% on the surface layer. This increase might be an effect of heterogeneities on the top of the soil deposit, resulting in wave scattering phenomena.

Finally, implications of the inverted soil models into the site response were addressed, by comparing the estimated stratigraphic amplification with the one observed at GVDA. In this study, the amplification is described as acceleration transfer function (TF), i.e. the ratio of the Fourier spectra between acceleration time histories at different depths. Specifically, empirical TFs between the surface sensor and the ones at 6 m and 15 m depth were considered, the values of which were taken from Vantassel and Cox [15]. The corresponding theoretical TFs were computed through linear visco-elastic simulations, assuming "within" conditions at each reference depth, for compatibility with empirical data. TFs were computed from MASW data and the invasive surveys mentioned above. Different testing procedures result in TFs with nonidentical location and amplitude of peaks, due to different V_S and D_0 values especially in the shallow layer. However, MASW data compare moderately well with the empirical TF when considering the shallower sensor (Fig. 5a), especially for the fundamental peak. On the contrary, the fitting quality for the fundamental mode is poor when the deeper sensor is adopted, although the compatibility slightly improves at high frequencies (Fig. 5b). However, this discrepancy may be an effect of inaccuracies in the low-frequency data recorded in the sensor at 15 m depth [15].

5 Conclusions

The present paper investigated the efficiency of surface wave analysis in estimating the small-strain damping ratio from a MASW survey carried out at the Garner Valley Downhole Array. First, uncertainties in the estimation of the Rayleigh wave phase velocity and attenuation were assessed, focusing on inter-method difference and on the effect of source characteristics. On the one side, all the considered approaches provide similar dispersion estimates, whereas some divergence is observed in attenuation data. Furthermore, the novel FDBFa method returns results compatible with other approaches, both in terms of mean and variability. As for the source effect, data from vibroseis and sledgehammer compare quite well, though the latter is characterized by larger variability. However, this result positively contributes to the capability of the sledgehammer for the attenuation estimate. This is helpful for ordinary applications, where high-energy sources are not typically available.

Then, reliable profiles of S-wave velocity and damping ratio were extracted from experimental data through an inversion process. The resulting models exhibit well-constrained velocity profiles, whereas damping ratios are more scattered, but a trend can still be identified. Such variability may be the combined effect of the large CoV in attenuation data and the limited wavelength range investigated, that prevent from properly constraining the inverted models. Nonetheless, the estimated amplification is compatible with empirical data and with results obtained from other surveys.

Future work will focus on an extended characterization of dissipation properties on the whole array. Furthermore, the possibility of extracting attenuation from ambient

noise data will be addressed, to better constrain estimated damping ratios at greater depths.

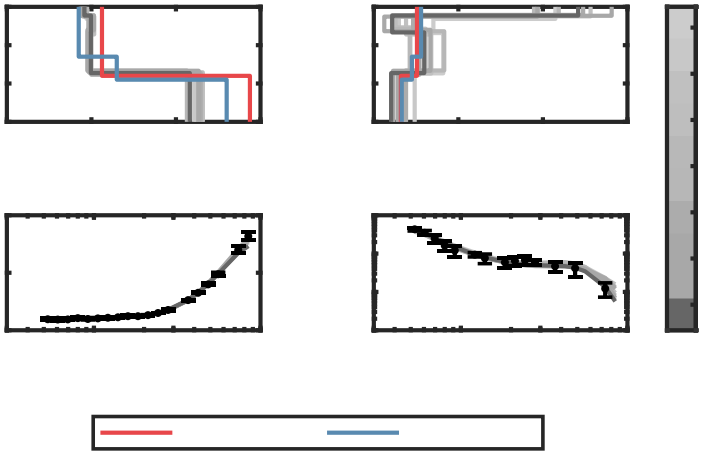

Fig. 4. Inverted S-wave velocity (a) and damping ratio profiles (b); c) Theoretical vs. experimental dispersion curves; d) Theoretical vs. experimental attenuation curves. Theoretical data correspond to the best fitting 10 models. Profiles obtained from a Down-Hole (DH) test [13] and PS suspension logging (PS) [11] are included, where D_0 was estimated through Darendeli's relationship [14].

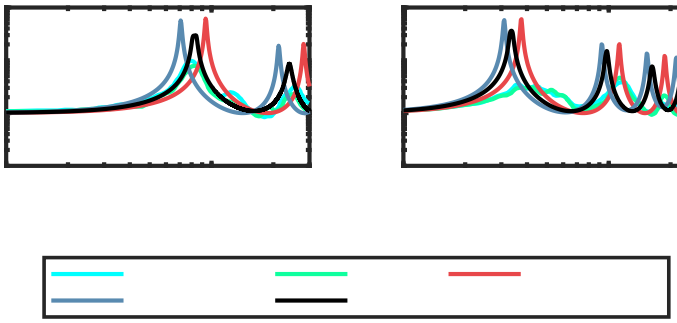

Fig. 5. Comparison between experimental transfer function (ETF, extracted from Vantassel and Cox [13]) and median theoretical transfer function for the best fitting 10 models in the inversion (MASW), for the reference depths of 6 m (a) and 15 m (b). Theoretical transfer functions obtained from results of a Down-Hole (DH) test [13] and PS suspension logging (PS) [11] are included, where D_0 was estimated through Darendeli's relationship [14]. Experimental data are labelled as North-South (NS) and East-West (EW), corresponding to the components of seismometer records from which they were derived.

6 Acknowledgements

The study was partially supported by the ReLUIS 3 project, funded by the Italian Civil Protection Agency. Data were extracted from the NSF Project "Collaborative Research:

3D Ambient Noise Tomography for Natural Hazards Engineering" grant CMMI-1931162. However, any opinions, findings, and conclusions or recommendations expressed in this material are those of the authors and do not necessarily reflect the views of the NSF. The seismic instruments were provided by IRIS through the PASSCAL Instrument Center at New Mexico Tech. Data collected will be available through the IRIS Data Management Center. The facilities of the IRIS Consortium are supported by the NSF SAGE Award under Cooperative Support Agreement EAR-1851048.

References

1. Foti, S., Aimar, M., Ciancimino, A.: Uncertainties in Small-Strain Damping Ratio Evaluation and Their Influence on Seismic Ground Response Analyses. In: Latest Developments in Geotechnical Earthquake Engineering and Soil Dynamics, 175-213. Springer (2021).
2. Thompson E. M., Baise L. G., Kayen R. E., Guzina B. B.: Impediments to predicting site response: seismic property estimation and modeling simplifications. Bulletin of the Seismological Society of America 99(5), 2927–2949 (2009).
3. Lai, C. G., Rix, G. J., Foti, S., Roma, V.: Simultaneous measurement and inversion of surface wave dispersion and attenuation curves. Soil Dynamics and Earthquake Engineering 22(9-12), 923-930 (2002).
4. UT Austin NHERI Experimental Facility, https://utexas.designsafe-ci.org/equipment-portfolio/, last accessed 2021/10/22.
5. Badsar, S. A., Schevenels, M., Haegeman, W., Degrande, G.: Determination of the material damping ratio in the soil from SASW tests using the half-power bandwidth method. Geophysical Journal International 182(3), 1493-1508 (2010).
6. Bergamo, P., Maranò, S., Imperatori, W., Hobiger, M., Fäh, D.: Wavefield decomposition technique applied to active surface wave surveys: towards joint estimation of shear modulus and dissipative properties of the near-surface. In: EPOS@ SERA "Strong Motion Site Characterization" workshop (2019).
7. Aimar, M.: Uncertainties in the Estimation of the Shear-Wave Velocity and the Small-Strain Damping Ratio from Surface Wave Analysis. Ph.D. Dissertation, Politecnico di Torino, Italy (2022) (In preparation).
8. Zywicki, D. J.: Advanced signal processing methods applied to engineering analysis of seismic surface waves, Ph.D. Dissertation, Georgia Institute of Technology, Georgia (1999).
9. Cox, B. R., Wood, C. M., Teague, D. P.: Synthesis of the UTexas1 Surface Wave Dataset Blind-Analysis Study: Inter-Analyst Dispersion and Shear Wave Velocity Uncertainty. In: Geo-Congress 2014 Technical Papers, Atlanta, GA, 2014, pp. 850–859.
10. Socco, L. V., Boiero, D.: Improved Monte Carlo inversion of surface wave data. Geophysical Prospecting 56(3), 357-371 (2008).
11. Steller, R.: New borehole geophysical results at GVDA. UCSB Internal report (1996).
12. Schevenels, M., Degrande, G., François, S.: EDT: An ElastoDynamics Toolbox for MATLAB. Computers & Geosciences 35(8), 1752-1754 (2009).
13. Gibbs, J. F.: Near-surface P- and S-wave velocities from borehole measurements near Lake Hemet, California. U.S. Geological Survey Open File Report (1989).
14. Darendeli, M. B.: Development of a new family of normalized modulus reduction and material damping curves. Ph.D. Dissertation, The University of Texas, Austin (2001).
15. Vantassel, J. P., Cox, B. R.: Multi-reference-depth site response at the Garner Valley Downhole Array. In: Proceedings of the VII ICEGE, 8 (2019).